JACS JOURNAL OF THE AMERICAN CHEMICAL SOCIETY

Article

Cite This: J. Am. Chem. Soc. 2018, 140, 974−983

pubs.acs.org/JACS

Monochromophoric Design Strategy for Tetrazine-Based Colorful Bioorthogonal Probes with a Single Fluorescent Core Skeleton

Youngjun Lee,[†] Wansang Cho,[†] June Sung,[‡] Eunha Kim,[*,‡] and Seung Bum Park[*,†,§]

[†]CRI Center for Chemical Proteomics, Department of Chemistry, Seoul National University, Seoul 08826, Korea

[‡]Department of Molecular Science and Technology, Ajou University, Suwon 16499, Korea

[§]Department of Biophysics and Chemical Biology, Seoul National University, Seoul 08826, Korea

Supporting Information

ABSTRACT: Fluorogenic bioorthogonal probes are ideal for fluorescent imaging in live cell conditions. By taking advantage of the dual functionality of tetrazine (Tz), as a bioorthogonal reaction unit as well as a fluorescence quencher, a fluorophore−Tz conjugate (FL_{Tz}) has been utilized for fluorescent live cell imaging via inverse electron-demand Diels−Alder (iEDDA) type bioorthogonal reactions. However, most FL_{Tz} strategies rely on a donor−acceptor-type energy transfer mechanism, which limits red-shifting of probes' emission wavelength without deterioration of the fluorescent turn-on/off ratio. To address this constraint, herein we present a monochromophoric design strategy for making a series of FL_{Tz}s spanning a broad range of emission colors. For the systematic comparison of design strategies with minimized structural differences, we selected indolizine-based emission-tunable Seoul-Fluor (SF) as a model fluorophore system. As a result, by inducing strong electronic coupling between Tz and π-conjugation systems of an indolizine core, we efficiently quench the fluorescence of SF−tetrazine conjugates (SF_{Tz}s) and achieved more than 1000-fold enhancement in fluorescence after iEDDA reaction with *trans*-cyclooctene (TCO). Importantly, we were able to develop a series of colorful SF_{Tz}s with a similar turn-on/off ratio regardless of their emission wavelength. The applicability as bioorthogonal probes was demonstrated with fluorescence bioimaging of innate microtubule and mitochondria using docetaxel−TCO and triphenylphosphonium−TCO in live cells without washing steps. We believe this study could provide new insight for the reliable and generally applicable molecular design strategy to develop bioorthogonal fluorogenic probes having an excellent turn-on ratio, regardless of their emission wavelength.

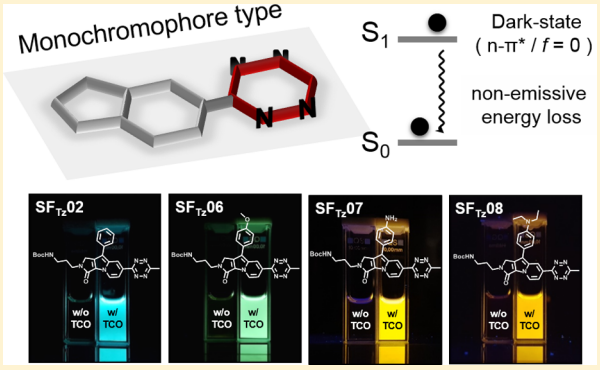

Fluorescent imaging techniques have revolutionized the way to understand biological systems at the nanoscopic,[1] microscopic,[2] and macroscopic levels.[3] To date, fluorescent proteins and immunofluorescence techniques have been most widely used for imaging a target of interest (TOI).[4] However, the requirement of genetic engineering, fixation, cell membrane penetration, or other treatment conditions makes these techniques unsuitable for imaging of innate proteins under a live cell environment, especially for primary cells or clinical samples. An alternative method is making a fluorescent conjugate, which binds specifically to the TOI protein.[5] The simplest approach for a fluorescent conjugate is the direct coupling of fluorochromes to ligands of TOI proteins, but this approach can reduce the binding affinity of ligand−fluorochrome probes or redirect these probes to off-target proteins in a nonspecific manner.[6] Moreover, extensive washing is required to remove an excess amount of fluorescent conjugates to get a higher signal-to-noise ratio. By taking advantage of bioorthogonal chemistry (highly specific and working in aqueous conditions),[7] researchers now can develop exquisite ligands for protein bioimaging with a minimal perturbation of original binding affinity, due to the much smaller size of bioorthogonal tags for the ligand modification compared to that of direct fluorophore ligation.[8]

Among various bioorthogonal reactions, recent advances in inverse electron-demand Diels−Alder (iEDDA) reaction received enormous attention because of its superior kinetics and specificity under physiological conditions.[9] Based on the dual functionality of tetrazine (Tz), a bioorthogonal reactive group[10] as well as a fluorescence quencher,[10e,f] a fluorophore−Tz conjugate (FL_{Tz}) has been at the center of attention.[8b,11] FL_{Tz}s can selectively react with a *trans*-cyclooctene (TCO)−ligand complex via an iEDDA reaction as a simultaneous bioorthogonal fluorogenic reaction, which allows fluorescence imaging of multiple intracellular proteins[8a,12] under live cell conditions without washing steps (Figure 1a).

Up to now, several approaches have been pursued to generate the FL_{Tz} having better turn-on efficiency with a wider range of fluorescent emission wavelengths.[9] From a molecular architectural point of view, the earlier version of FL_{Tz} has aliphatic linkers

Received: September 30, 2017
Published: December 14, 2017

DOI: 10.1021/jacs.7b10433
J. Am. Chem. Soc. 2018, 140, 974−983

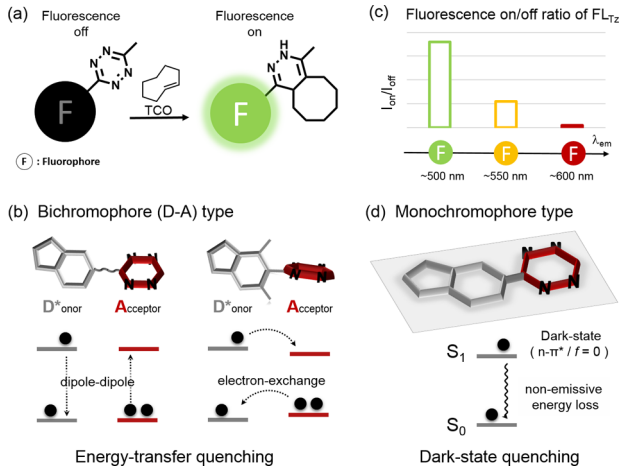

Figure 1. (a) Schematic representation of a fluorescence turn-on event of a fluorophore−tetrazine conjugate (FL_{Tz}), induced by bioorthogonal cycloaddition reaction with *trans*-cyclooctene (TCO). (b) Bichromophore-type FL_{Tz} quenched by dipole−dipole energy transfer (left) or electron-exchange energy transfer (right). (c) Reported trends of change in fluorescence on/off ratio of FL_{Tz} depending on the emission wavelengths of the fluorophores. (d) Monochromophore type FL_{Tz}, quenched by an optically inactive S_0−S_1 transition (dark-state quenching).

between the fluorophore (donor) and Tz (acceptor) for simple conjugation,[11a] and the fluorescence of FL_{Tz} is assumed to be quenched by transferring the fluorophore's excited energy to the Tz quencher via a long-range dipole−dipole interaction, also known as Förster resonance energy transfer (FRET) (Figure 1b, left).[13] A few years later, a new type of molecular design emerged via direct conjunction (without aliphatic linkers) of Tz to the flat organic fluorophores in an out-of-plane shape, due to the steric hindrance from adjacent substituents,[11b−d] which is known as a through-bond energy transfer (TBET) strategy.[14] Considering the close proximity (<10 Å) between the donor (D) and acceptor (A) along with electronically decoupled structures, an excited donor of a TBET pair might transfer its energy to the Tz quencher via a short-range electron-exchange mechanism (Figure 1b, right).[15] Although FRET- and TBET-based strategies were successfully applied to several fluorochromes for the development of fluorogenic FL_{Tz}s, a significant decrease in fluorescence turn-on/off ratio at longer emission wavelengths is a problem yet to be solved (Figure 1c). Therefore, there is a high demand in alternative molecular design strategies for an FL_{Tz} having a high turn-on/off ratio independent of the FL_{Tz}'s emission wavelength, to succeed in high-quality multiplex fluorescent imaging of TOI proteins in live cells.

Herein, we report the development of SF_{Tz}, a new series of FL_{Tz} fluorogenic probes using an emission-tunable Seoul-Fluor (SF) fluorescent core skeleton[16] via a monochromophoric design strategy (Figure 1d). Based on our understanding of the structure−photophysical property relationship of the SF system, we designed SF_{Tz} analogues through Tz modification at the R^1, R^2, or R^3 position of SF to systematically compare TBET-, FRET-, or monochromophore-based FL_{Tz}s. SF_{Tz}s have fast reaction kinetics with TCO in aqueous conditions and turn-on/off ratios up to 1000-fold with full-visible-color emission ranges. With SF_{Tz}s, we successfully visualized innate microtubules and mitochondria using TCO−ligand complexes in live cell conditions without washing steps. To the best of our knowledge, this is the first report about FL_{Tz} turn-on probes with a single core skeleton covering a full range of visible color, for the washing-free fluorescent live-cell imaging of innate TOI proteins and intracellular organelles.

RESULTS AND DISCUSSION

Initial Design and Synthesis. Many of blue or green color-emitting FL_{Tz}s showed a remarkable turn-on/off ratio by taking advantage of a donor−acceptor (D−A)-type bichromophoric design strategy.[11b−d] However, orange-, red-, or far-red-emitting FL_{Tz}s suffered drastic deterioration of their on/off ratio,[11a,c,f] implying the turn-on/off efficiency of D−A-type FL_{Tz} pairs is presumably dependent on the energy level of donor fluorophores.[17] In other words, fluorophores with red-shifted emission wavelengths (>550 nm) have a lower efficiency of transferring their excited energy to Tz, causing more severe residual background fluorescence than that of short-wavelength FL_{Tz}, in the case of a D−A-type bichromophoric system. To overcome this wavelength-dependent quenching efficiency, we envisioned an alternative molecular design approach, the monochromophoric strategy, which features strong electronic coupling between Tz and fluorophores for the development of super-dark FL_{Tz}.

Many Tz derivatives, even with multiple aromatic groups, are known to be nonfluorescent.[18] Once excited, Tz derivatives should undergo a nonradiative energy decay process due to the lowest lying dark state at S_1 (dark-state quenching),[19] presumably originated from a nonradiative n → π^* transition.[20] In this context, we hypothesized that unlike previous energy transfer quenching in a D−A-type (bichromophoric) FL_{Tz} system, which is sensitive to the donor's energy level, the monochromophoric FL_{Tz} system would have an inherent n → π^* transition stemming from Tz, and it could allow highly efficient dark-state quenching independent from the donor's energy level. After the spontaneous iEDDA reaction of Tz with TCO, irreversible releases of two nitrogen atoms from Tz would cause huge changes in the nonbonding orbitals of the monochromophoric FL_{Tz} system. Subsequently, the lowest lying nonradiative

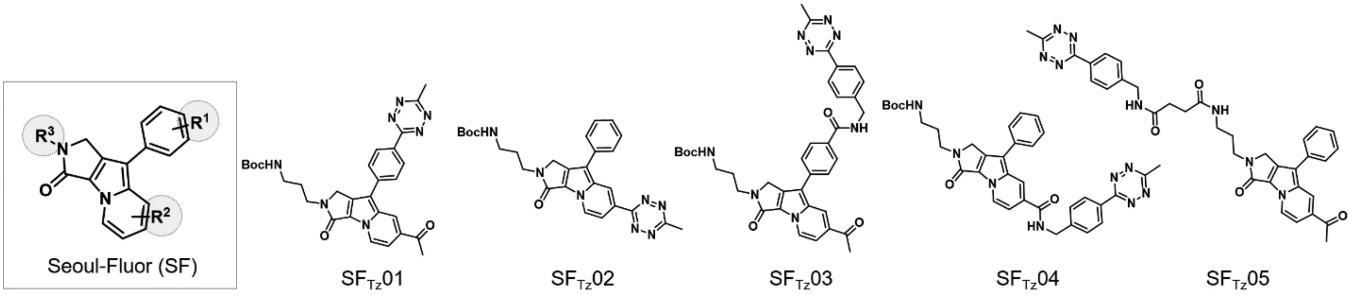

Figure 2. Molecular structures of Seoul-Fluor (SF) and SF−tetrazine conjugates (SF_{Tz}s).

DOI: 10.1021/jacs.7b10433
J. Am. Chem. Soc. 2018, 140, 974−983

n → π* transition might vanish in this state, which allows fluorescence turn-on via an optically active π → π* transition originating from the embedded fluorophores after iEDDA reaction. To prove this hypothesis, we designed and synthesized a series of FL_{Tz} derivatives sharing a single core skeleton, an emission-tunable indolizine-based Seoul-Fluor, to minimize other factors from resulting in structural differences.

Owing to its full-color-tunable fluorescence property and synthetic versatility, the SF scaffold can be an ideal fluorophore system to test our molecular design strategy. For the systematic comparison of each design strategy of FL_{Tz} with the SF scaffold, we utilized three distinct modification sites, the R^1, R^2, and R^3 positions of the SF scaffold. As shown in Figure 2, $SF_{Tz}01$ and $SF_{Tz}02$ were designed to incorporate the Tz chromophore without aliphatic linkers at the R^1 and R^2 positions, respectively. For $SF_{Tz}01$, a Tz-containing aryl moiety at the R^1 position can be geometrically tilted from the indolizine π-system,[16d] leading to decoupling of the π-systems between indolizine and Tz, which is a hallmark of a TBET-based FL_{Tz}. Special attention was paid toward the molecular architecture of $SF_{Tz}02$, because the π-conjugation systems of two chromophores, indolizine and Tz, can be strongly coupled with each other due to the negligible rotational barrier of the single bond between indolizine and Tz. Thus, we hypothesized $SF_{Tz}02$ might behave as a monochromophoric FL_{Tz}. In the case of $SF_{Tz}03$–05, we introduced Tz to the SF scaffold through aliphatic linkers at the R^1, R^2, and R^3 positions, respectively, as analogues of FRET-based FL_{Tz}s.

For the synthesis of $SF_{Tz}01$ (Scheme 1), we used palladium-mediated C–H activation of the indolizine core and incorporated

Scheme 1. Synthetic Scheme of $SF_{Tz}01$–03

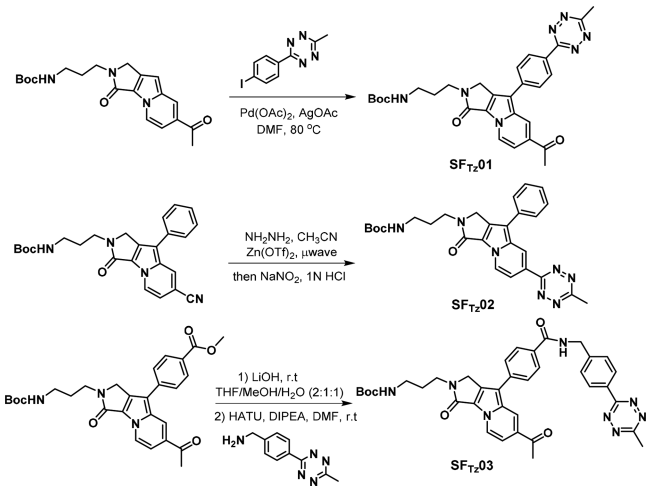

a Tz moiety at the R^1 position in the presence of 3-(4-iodophenyl)-6-methyl-1,2,4,5-tetrazine and $Pd(OAc)_2$ with AgOAc.[16d] $SF_{Tz}02$ was prepared via direct conversion of a nitrile group at the R^2 position of the indolizine moiety into Tz under microwave irradiation using NH_2NH_2, acetonitrile, and $Zn(OTf)_2$, followed by an acid-mediated oxidation step with $NaNO_2$.[21] In the case of $SF_{Tz}03$, $SF_{Tz}04$, and $SF_{Tz}05$, the carboxyl acid moiety at the R^1, R^2, or R^3 position of the corresponding SFs was coupled with a Tz moiety containing an aliphatic amine, 4-(6-methyl-1,2,4,5-tetrazin-3-yl)benzylamine, with the aid of HATU and DIPEA. The final SF_{Tz} products were thoroughly purified by preparative high-performance liquid chromatography before checking their photophysical properties. More detailed information on the synthetic procedure and full characterization of all new compounds are available in the Supporting Information.

Change in Absorption Property of $SF_{Tz}01$–05 upon TCO Cycloaddition Reaction. To investigate the effect of the molecular design on the electronic orthogonality between indolizine and Tz, we checked absorption spectra of SF_{Tz}s before and after the bioorthogonal reaction with TCO. Before the reaction with TCO, we observed two different absorption peaks around 400–420 nm and 500–550 nm from $SF_{Tz}01$, $SF_{Tz}03$, $SF_{Tz}04$, and $SF_{Tz}05$ (Figure 3, gray line). On the contrary, $SF_{Tz}02$ has an absorption peak around 400–420 nm, but indistinguishable absorption maxima around 500–550 nm (Figure 3c, gray line). Considering Tz analogues generally have a distinct weak absorption peak around 500–550 nm (Figure 3a, gray line),[18b,20] this observation indicates that $SF_{Tz}02$ has stronger coupled states between SF and Tz than others.

More clearly, the electronic orthogonality of SF_{Tz} analogues could be confirmed by analyzing absorption changes after iEDDA reaction with TCO. If Tz and the fluorophore have two independent and electronically decoupled states, the cycloaddition reaction of SF_{Tz} with TCO will cause independent dissipation of the absorption peak around 500–550 nm, which is originated from Tz's absorption, while most of absorption patterns in other wavelength ranges should be intact. On the other hand, if Tz and indolizine are strongly coupled and act as a single chromophore, the iEDDA reaction with TCO will lead to an overall hypsochromic shift in absorption spectra due to the reduction of the π-conjugation length. After the bioorthogonal reaction with TCO, $SF_{Tz}01$, $SF_{Tz}03$, $SF_{Tz}04$, and $SF_{Tz}05$ showed marginal to negligible changes in absorption spectra except for a clear disappearance of absorption around 500–550 nm (Figure 3, inset graphs). As described earlier, FRET-based $SF_{Tz}03$–$SF_{Tz}05$ were constructed via the conjugation of two chromophores, indolizine and Tz, with aliphatic linkers. Therefore, electronically decoupled states between SF and Tz were expected, which leads to negligible changes in absorption spectra of $SF_{Tz}03$–$SF_{Tz}05$ after iEDDA reaction. In the case of TBET-based $SF_{Tz}01$, we proposed that the Tz moiety at the R^1 position is geometrically tilted and electronically decoupled from the π-system of indolizine, which was strongly supported by marginal changes in the absorption spectrum of $SF_{Tz}01$ around 400 nm (indolizine's π → π* absorption band) after the iEDDA reaction. These observations confirmed that $SF_{Tz}01$ and $SF_{Tz}03$–$SF_{Tz}05$ have electronically decoupled π-systems between two chromophores. On the other hand, drastic overall changes of $SF_{Tz}02$ in the absorption spectra and hypsochromic shift of the absorption maximum (from 415 to 386 nm) upon TCO treatment clearly indicate that the monochromophoric molecular design of $SF_{Tz}02$ results in strong electronic coupling between the two chromophores, indolizine and Tz. Collectively, we were convinced that the electronic orthogonality of the π-conjugation system between Tz and indolizine is highly dependent on the applied molecular design strategies.

Change in Fluorescence Property of $SF_{Tz}01$–05 upon Cycloaddition Reaction with TCO. Next, we investigated fluorescence changes of $SF_{Tz}01$–05 by comparing the emission spectra before and after (when reaching the maximum intensity in fluorescence) reacting with TCO. Interestingly, the strong electronically coupled $SF_{Tz}02$ results in remarkable enhancement of turn-on/off ratio via complete dark-state quenching (Figure 4b). As shown in Table 1, $SF_{Tz}02$ showed a completely quenched fluorescence property (quantum yield: 0.2%), while

DOI: 10.1021/jacs.7b10433
J. Am. Chem. Soc. 2018, 140, 974–983

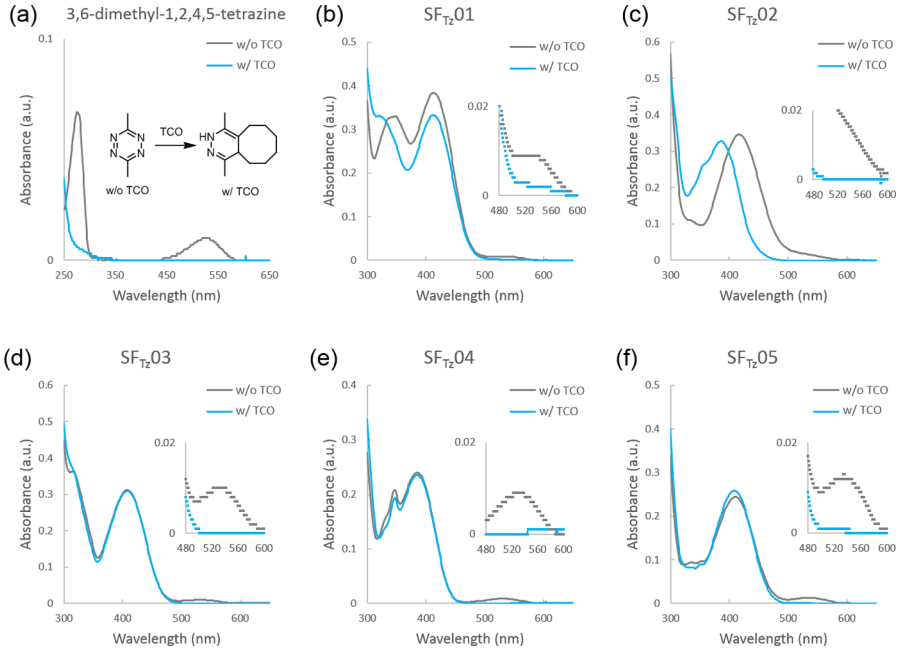

Figure 3. Changes in absorption spectra for Tz-containing molecules before (gray line) and after (blue line) the reaction with TCO: (a) 3,6-Dimethyl-1,2,4,5-tetrazine, (b) SF$_{Tz}$01, (c) SF$_{Tz}$02, (d) SF$_{Tz}$03, (e) SF$_{Tz}$04, (f) SF$_{Tz}$05. All spectra were measured in an acetonitrile/H_2O (1:1 v/v) mixture at room temperature. The final concentration of dye and TCO was 20 μM and 200 μM, respectively.

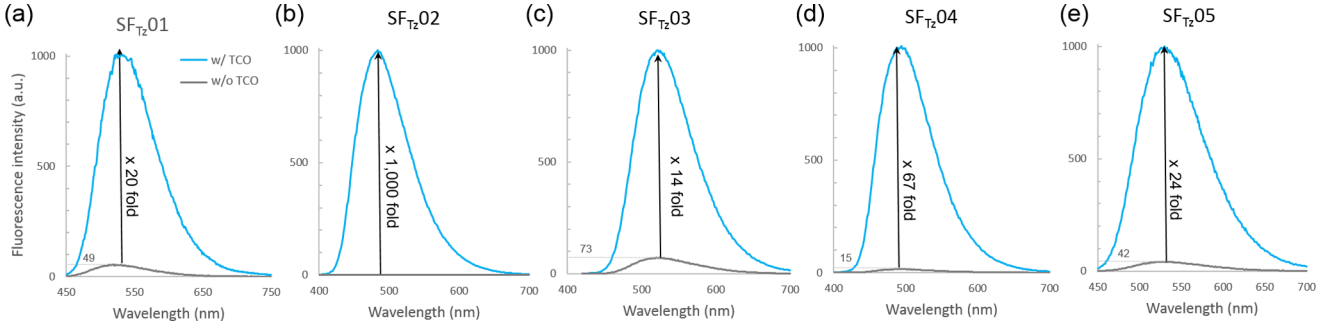

Figure 4. Changes in emission spectra for SF$_{Tz}$01–SF$_{Tz}$05 before (gray line) and after (blue line) the reaction with TCO: (a) SF$_{Tz}$01, (b) SF$_{Tz}$02, (c) SF$_{Tz}$03, (d) SF$_{Tz}$04, (e) SF$_{Tz}$05. All spectra were measured in an acetonitrile/H_2O (1:1 v/v) mixture at room temperature. Final concentration of dye and TCO was 20 μM and 200 μM, respectively. Each SF$_{Tz}$ was excited at the corresponding largest excitation maxima of the fluorogenic form.

Table 1. Photophysical Properties for SF$_{Tz}$s before and after the Reaction with *trans*-Cyclooctene (TCO)

probe	Φ_{off} [a]	k_2 [b] (M^{-1} s^{-1})	λ_{ex} [c] (nm)	λ_{em} [d] (nm)	Φ_{on} [e]	fold (on/off) [f]
SF$_{Tz}$01	0.011	21	416	532	0.168	20
SF$_{Tz}$02	0.002	24	375	484	0.683	>1000
SF$_{Tz}$03	0.042	15	401	522	0.583	14
SF$_{Tz}$04	0.012	15	375	493	0.616	67
SF$_{Tz}$05	0.017	8.5	401	530	0.325	24

[a,e]Φ_{off} and Φ_{on} denote absolute quantum yield of the SF$_{Tz}$ and SF$_{Py}$ form, respectively. [b]Second-order rate constant measured at 20 °C. [c]The largest excitation maxima at the given maximal emission wavelength. [d]Maximal emission wavelength. [f]Fold enhancement of fluorescence intensity upon reaction with TCO. All experimental data were measured in an acetonitrile/H_2O (1:1 v/v) mixture. Final concentration of SF$_{Tz}$ and TCO was 20 μM and 200 μM, respectively. λ_{em}, Φ_{off}, and Φ_{on} were measured at the corresponding λ_{ex} of each SF$_{Tz}$.

others showed residual fluorescence (quantum yield: up to 4%) before reaction with TCO. Consequently, the residual off-state fluorescence of those FRET- or TBET-type SF$_{Tz}$s lead to a moderate on/off enhancement (10–70-fold) for SF$_{Tz}$01 and SF$_{Tz}$03–05, but superdark quenching of SF$_{Tz}$02 leads to an exceptional enhancement, more than 1000-fold, of the fluorescence on/off signal. This result suggests that our monochromophoric design strategy can generate a series of effectively quenched fluorophores by direct conjugation of Tz to the π-conjugated core structure of the fluorophore, which prompted us to develop a colorful series of monochromophoric SF$_{Tz}$s with ensured quenching efficiency even at a longer emission wavelength.

Reaction Kinetics. Next, we evaluated the reaction kinetics of the SF$_{Tz}$ series by tracking the change in fluorescence intensity over time, after treatment with TCO. As shown in Table 1 and Figure S1, the entire SF$_{Tz}$ series showed fast reaction kinetics ($k_2 \approx 10$ M^{-1} s^{-1}) in 1:1 acetonitrile/water conditions, which is comparable with widely used bioorthogonal reactions, such as copper-catalyzed azide–alkyne cycloadditions (CuAAC, >10 M^{-1} s^{-1})[22] or photoclick cycloadditions (<60 M^{-1} s^{-1}).[22b,23]

Rational Expansion of Multicolor SF$_{Tz}$s Based on a Monochromophoric Strategy. Based on our knowledge about emission modularity of SF,[16b] we designed a series of

DOI: 10.1021/jacs.7b10433
J. Am. Chem. Soc. 2018, 140, 974–983

$SF_{Tz}02$ analogues to span a wide emission range simply by changing the electronic nature of substituents at the R^1 position of monochromophoric SF_{Tz}. As shown in Figure 5a, we

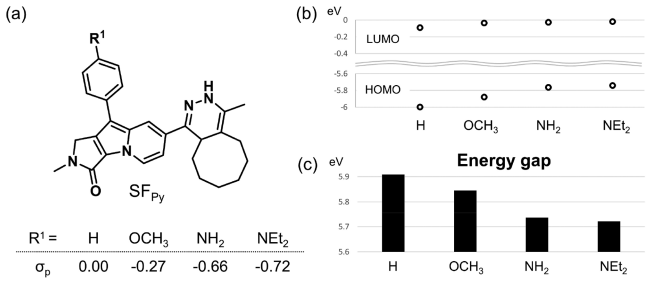

Figure 5. (a) Structure of representative fluorescence on-state SF analogue, SF_{Py}, generated from cycloaddition reaction of $SF_{Tz}02$ with TCO and Hammett constant values (σ_p) of H, OCH_3, NH_2, and NEt_2 functional groups. (b) Calculated HOMO and LUMO energy values (DFT, CAM-B3LYP/6-31G*) of SF_{Py} having H, OCH_3, NH_2, and NEt_2 groups at the R^1 position. (c) Changes in the HOMO−LUMO energy gap of SF_{Py}s with corresponding functional groups at the R^1 position.

introduced electron-donating substituents guided by the Hammett constant[24] [methoxy (σ_p = −0.27), amino (−0.66), and diethylamino group (−0.72)] at the R^1 position of SF_{Py}—the corresponding iEDDA reaction product of SF_{Tz} with TCO having a 1,4-dihydropyridazine moiety—to induce a bathochromic shift of the emission wavelength of SF_{Tz}−TCO adducts. The trend in emission wavelength changes of SF_{Py} analogues was predicted by density functional theory (DFT) calculation at the CAM-B3LYP/6-31G* level.[25] It is worth mentioning that during the continuous monitoring of the fluorogenic reaction for $SF_{Tz}02$ with TCO using mass spectroscopy, we observed a progressive disappearance of the mass peak of $SF_{Tz}02$ until the fluorescence signal reached a maximum, along with the gradual emergence of a new mass peak, which is matched with that of two different types of SF_{Tz}-TCO adducts, 1,4- and 4,5-dihydropyridazine forms. In this study, we mainly considered the 1,4-dihydropyridazine isomer as a representative fluorogenic SF_{Py} on the basis of previous reports.[11a,b,g] As shown in Figure 5b, electron-donating groups at the R^1 position can raise the energy level of the highest occupied molecular orbital (HOMO) more than that of the lowest unoccupied molecular orbital (LUMO). Therefore, the substitution of methoxy, amino, and diethylamino groups results in the reduced HOMO−LUMO energy gap of the SF system (Figure 5c and Table S1), which is expected to induce a bathochromic shift of emission wavelength compared to that of $SF_{Tz}02$. We also observed similar trends in HOMO−LUMO energy gaps according to the changes of substituents at the R^1 position using 4,5-dihydropyridazine form as SF_{Py} analogues (Figure S2 and Table S2).

Accordingly, we synthesized $SF_{Tz}06$ (R^1 = methoxy; calculated energy gap = 5.846 eV), $SF_{Tz}07$ (amino; 5.736 eV), and $SF_{Tz}08$ (diethylamino; 5.722 eV) to generate a multicolor set of bioorthogonal SF_{Tz} probes (Figure 6a). The synthetic procedure for these analogues was identical to that of $SF_{Tz}02$ (see Supporting Information). With these new analogues in hand, we first evaluated their electronic orthogonality between indolizine and Tz by checking the changes in absorption spectra, before and after TCO treatment (Figure 6b). Similar to $SF_{Tz}02$, all three compounds showed distinct hypsochromic shifts of absorption maxima (425 → 393, 436 → 399, and 457 → 409 nm for $SF_{Tz}06$, $SF_{Tz}07$, and $SF_{Tz}08$, respectively), which clearly

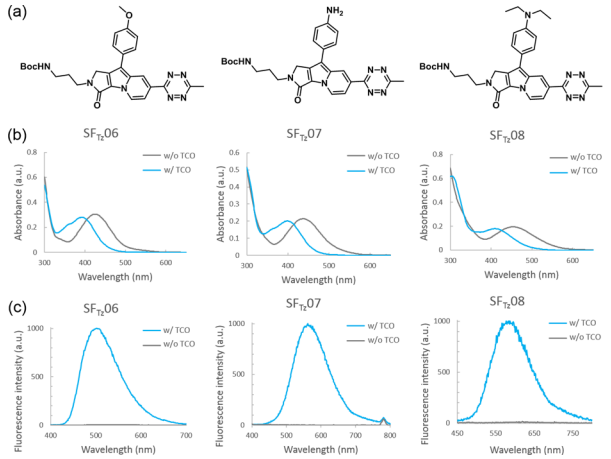

Figure 6. (a) Molecular structures of $SF_{Tz}06$ (left), $SF_{Tz}07$ (middle), and $SF_{Tz}08$ (right). (b) Changes in absorption spectra for $SF_{Tz}06$−08, before (gray) and after (blue) the reaction with TCO. (c) Changes in emission spectra for $SF_{Tz}06$−08, before (gray) and after (blue) the reaction with TCO. Final concentration of dye and TCO was 20 μM and 200 μM, respectively. Each SF_{Tz} was excited at the corresponding largest excitation maxima of the fluorogenic form.

suggested strong electronic coupling between Tz and the indolizine aromatic π-system. Upon the reaction with TCO, newly synthesized SF_{Tz}s showed decent reaction kinetics (>20 M^{-1} s^{-1}), similar to that of $SF_{Tz}02$ (Figure S3). Emission maxima of $SF_{Tz}06$ (505 nm), $SF_{Tz}07$ (562 nm), and $SF_{Tz}08$ (581 nm) were well matched with DFT calculations (Figures S4 and S5), and the resulting monochromophoric SF_{Tz}s, including $SF_{Tz}02$, cover blue to orange visible-color emission (Figure 7 and Table 2).

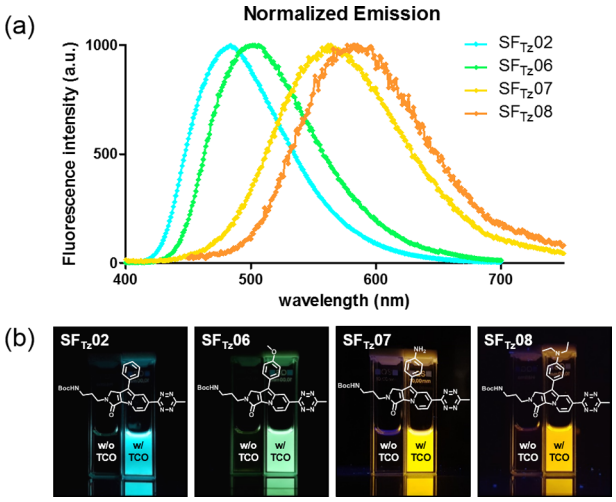

Figure 7. (a) Normalized emission spectra of $SF_{Tz}02$, $SF_{Tz}06$, $SF_{Tz}07$, and $SF_{Tz}08$ after the reaction with TCO (SF_{Tz}s 20 μM, TCO 200 μM). (b) Photographic images of each SF_{Tz} irradiated at 365 nm, before and after reacting with TCO.

The most remarkable achievement of our monochromophoric SF_{Tz} system is the complete quenching of residual fluorescence at the off-state, regardless of emission wavelength (Figure 6c and Table 2). Due to complete dark-state quenching, the fluorescence on/off ratio of all monochromophoric SF_{Tz}s showed remarkable triple or quadruple-digit-fold enhancement (600−1000-fold), independent from their emission wavelength, even in the case of $SF_{Tz}08$, with an emission wavelength of >580 nm (Table 2).

DOI: 10.1021/jacs.7b10433
J. Am. Chem. Soc. 2018, 140, 974−983

Table 2. Photophysical Properties for Monochromophoric SF_{Tz}s before and after the Reaction with TCO

probe	Φ_{off} [a]	k_2 [b] (M^{-1} s^{-1})	λ_{ex} [c] (nm)	λ_{em} [d] (nm)	Φ_{on} [e]	fold (on/off) [f]
SF_{Tz}02	0.002	24	375	484	0.683	>1000
SF_{Tz}06	0.001	23	383	505	0.485	>1000
SF_{Tz}07	0.002	22	390	562	0.064	>600
SF_{Tz}08	0.001	22	401	581	0.045	>600

[a,e]Φ_{off} and Φ_{on} denote absolute quantum yield of the SF_{Tz} and SF_{Py} form, respectively. [b]Second-order rate constant measured at 20 °C. [c]The largest excitation maxima at the given maximal emission wavelength. [d]Maximal emission wavelength. [f]Fold enhancement of fluorescence intensity upon reaction with TCO. All experimental data were measured in an acetonitrile/H_2O (1:1 v/v) mixture. Final concentration of SF_{Tz} and TCO was 20 μM and 200 μM, respectively. λ_{em}, Φ_{off}, and Φ_{on} were measured at the corresponding λ_{ex} of each SF_{Tz}.

TD-DFT Calculation. To decipher the fluorescence turn-on mechanism and photophysical property of SF_{Tz}02 and its analogues (SF_{Tz}06–08), we conducted time-dependent (TD)-DFT calculations (CAM-B3LYP/6-31G*)[25] with energy-minimized conformers of SF_{Tz}s and their corresponding iEDDA reaction products having the 1,4-dihydropyridazine form (SF_{Py}). Our major concern was the probability of optical S_0–S_1 transition at the lowest lying first singlet excited state, which is known as the most important electronic state for fluorescence phenomenon according to Kasha's rule.[26] In this regard, geometry optimization of the first excited state for monochromophoric SF_{Tz}s and SF_{Py}s was conducted. Then, molecular orbitals and oscillator strength values (f)[27]—the optical transition probability—between S_0 and S_1 states were investigated using quantum mechanical calculations. As shown in Figure 8a and Table S3, the dominant orbitals contributing to the S_0–S_1 transition of all monochromophoric SF_{Tz}s were expected to have an n → π^* type transition.[20] Based on the orbital distribution of the lowest first excited state of all SF_{Tz}s, we confirmed that nonbonding orbitals from the nitrogen-atom-rich Tz significantly contribute to the n → π^* transition within the molecule. On top of that, the f values for all SF_{Tz}s are very close to zero, suggesting that optical transition between S_0 and S_1 is almost forbidden.[27] Therefore, low optical transition possibility for the S_0–S_1 transition strongly indicates that monochromophoric SF_{Tz}s would lose their excited energy via a nonradiative decay process. Note that this is a completely different quenching mechanism from TBET- or FRET-based systems, whose quenching performance is governed by energy transfer efficiency from the excited fluorophore to the electronically decoupled Tz quencher.

After the cycloaddition reaction of SF_{Tz} with TCO, removal of two nitrogen atoms as well as extinction of the aromatic system of Tz might cause a huge transformation of nonbonding orbitals of SF_{Tz}. Therefore, the optically inactive n → π^* transition at the lowest lying state is no longer valid after iEDDA reaction, but the π → π^* transition becomes the most important transition between the S_0 and S_1 states in all SF_{Py}s (Figure 8b and Table S4). Besides, f values for the S_0–S_1 transition in SF_{Py}s (from 0.41 to 0.53) are significantly higher than that of the S_0–S_1 transition in SF_{Tz}s (from 0.0031 to 0.0040). In other words, radiative energy

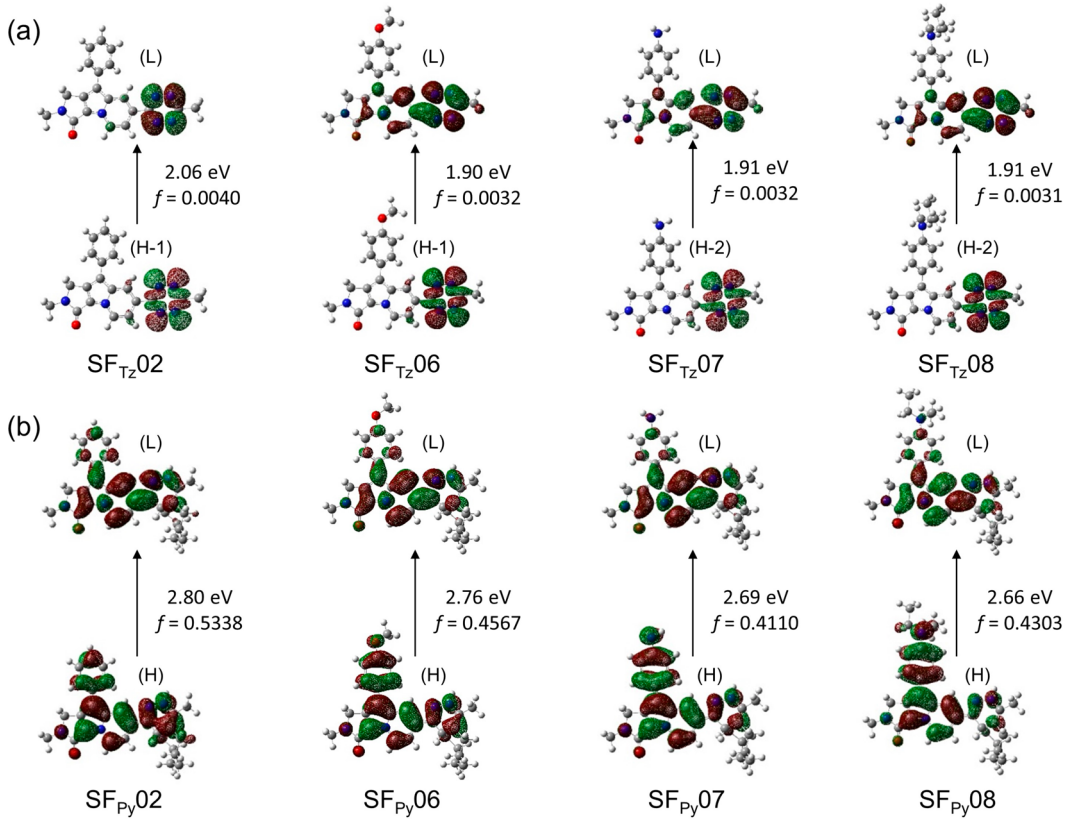

Figure 8. Molecular orbital distribution, vertical transition energy, and oscillator strength values (f) of SF_{Tz}02, SF_{Tz}06, SF_{Tz}07, and SF_{Tz}08, obtained by TD-DFT calculation (CAM-B3LYP/6-31G*) of the corresponding first excited-state optimized structures. (a) Quenched SF_{Tz} compounds before the reaction with TCO; (b) fluorogenic SF_{Py} products after the formation of TCO-adducts. The main contributing orbital of S_0–S_1 for each compound is illustrated. H and L stand for HOMO and LUMO, respectively.

DOI: 10.1021/jacs.7b10433
J. Am. Chem. Soc. 2018, 140, 974–983

loss of excited fluorophores becomes "allowed" after iEDDA reaction, and it makes SF_{Py}s fluorescent. We also observed almost identical results in the case of the 4,5-dihydropyridazine isomer as SF_{Py}s (Figure S6 and Table S5). In summary, computational calculation indicates that direct incorporation of Tz to SF makes the optically inactive n → π* transition (low *f* value) the major S_0-S_1 transition for SF_{Tz}s, which quenches the fluorescence process of chromophores. Destruction of Tz in SF_{Tz}s, induced by bioorthogonal iEDDA reaction with TCO, makes the optically active π → π* transition dominant (high *f* value) for the S_0-S_1 transition in SF_{Py}s, which turns on the molecules' fluorescence.

Direct Comparison of Mono- vs Bichromophoric SF_{Tz}s with Long Emission Wavelength. Next, we pursued direct comparison of the mono- vs bichromophoric design strategy by analyzing the turn-on/off ratio at the longer emission wavelength. For the comparison with SF_{Tz}08, the representative long-wavelength compound for monochromophoric SF_{Tz}, we simply introduced an electron-donating diethylamino group at the R^1 position of SF_{Tz}04 and SF_{Tz}05, to yield SF_{Tz}09 and SF_{Tz}10, respectively, as representative long-wavelength bichromophoric SF_{Tz}s (Figure 9). It turns out that after TCO treatment, electronically decoupled bichromophoric systems, SF_{Tz}09−10, showed noticeable depreciation of turn-on/off ratio (67- → 30-fold for SF_{Tz}04 → SF_{Tz}09 and 25- → 3-fold for SF_{Tz}05 → SF_{Tz}10) as the fluorophore's emission coverage was shifted to the longer emission area (Table 1, Table 3, Figure S7, and Figure S8).

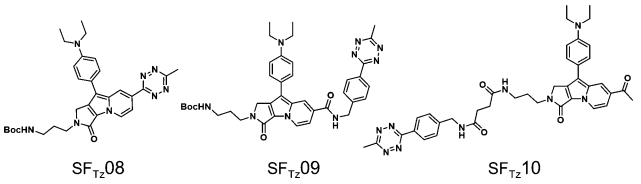

Figure 9. Molecular structures of SF_{Tz}08, SF_{Tz}09, and SF_{Tz}10 for the direct comparison of mono- and bichromophoric design strategies on SF_{Tz}. SF_{Tz}08, SF_{Tz}09, and SF_{Tz}10 are designed as long-emission-wavelength analogues for SF_{Tz}02 (monochromophoric SF_{Tz}) and SF_{Tz}04−05 (bichromophoric SF_{Tz}), respectively.

Table 3. Photophysical Properties of SF_{Tz}s before and after the Reaction with TCO

probe	Φ_{off} [a]	k_2 [b] (M^{-1} s^{-1})	λ_{ex} [c] (nm)	λ_{em} [d] (nm)	Φ_{on} [e]	fold (on/off) [f]
SF_{Tz}08	0.001	22	401	581	0.045	>600
SF_{Tz}09	0.005	15	418	608	0.016	30
SF_{Tz}10	0.013	1.2	438	625	0.028	3

[a,e]Φ_{off} and Φ_{on} denote absolute quantum yield of the SF_{Tz} and SF_{Py} form, respectively. [b]Second-order rate constant measured at 20 °C. [c]The largest excitation maxima at the given maximal emission wavelength. [d]Maximal emission wavelength. [f]Fold enhancement of fluorescence intensity upon reaction with TCO. Experimental data were measured in an acetonitrile/H_2O (1:1 v/v) mixture for SF_{Tz}08 and SF_{Tz}09 and in acetonitrile for SF_{Tz}10. Final concentration of SF_{Tz} and TCO was 20 μM and 200 μM, respectively. λ_{em}, Φ_{off}, and Φ_{on} were measured at the corresponding λ_{ex} of each SF_{Tz}.

On the contrary, the monochromophoric design strategy allowed SF_{Tz}08 to preserve compelling turn-on/off efficiency (over 600-fold), comparable to that of SF_{Tz}02 (over 1000-fold), at the long emission area. The slight reduction in turn-on/off ratio of SF_{Tz}08 might originate from the innate low quantum yield of its fluorogenic form. Collectively, this comparison experiment demonstrated the unique advantage of monochromophoric design strategy, which guarantees excellent fluorescence off/on ratio, independent from the emission wavelength of fluorophores. By taking advantage of the wavelength-independent quenching mechanism, different from conventional energy-transfer-type quenching (FRET or TBET), the monochromophoric approach could provide a robust and generally applicable molecular design strategy for the development of multicolor bioorthogonal fluorogenic probes with high turn-on ratio.

Bioapplication. Lastly, we applied SF_{Tz}02 and SF_{Tz}08 for cellular imaging to demonstrate the usefulness of SF_{Tz}s as multicolor bioorthogonal fluorogenic imaging probes. For the practical usage of SF_{Tz} probes, we changed the R^3 position of SF system—proven as orthogonal to the fluorescence property[16c,e]—by introducing a water-soluble moiety such as piperazine or carboxyl group to yield SF_{Tz}02* and SF_{Tz}08*, respectively (Figure S9). We first used docetaxel−TCO conjugate (Dox−TCO) for fluorescent bioimaging of microtubules (Figure 10). HeLa human cervical carcinoma cells were fixed and incubated with Dox−TCO for 1 h and washed briefly with PBS. Immediately after the addition of SF_{Tz}02* or SF_{Tz}08* to the cells, a bright cytoplasmic fluorescent signal was generated and the intracellular fluorescent images resembled typical spindle structures of microtubules (Figure 10b,d). Control experiments confirmed that there is a negligible background signal inside the cells and no background signal outside of the cells even with longer exposure time (Figure 10a,c). Therefore, we could achieve a sharp contrast in fluorescent signal between the cytoplasm and outside of fixed cells without washing steps to remove excess SF_{Tz} probes. Further immunofluorescence with α-tubulin antibody confirmed the specific staining of microtubules with Dox−TCO/SF_{Tz}s (Figure 10e−h).

Considering the importance of mitochondrial phenotyping,[28] we then explored the use of SF_{Tz}s in fluorescence imaging of mitochondria in live cells (Figure 11). After 1 h of incubation in the presence or absence of triphenylphosphonium (TPP)−TCO, HeLa cells were washed and treated with SF_{Tz}02* or SF_{Tz}08*. In the absence of TPP-TCO, no specific staining of mitochondria nor background signal was observed, even without washing steps (Figure 11a,i). On the other hand, TPP-TCO/SF_{Tz}02* or TPP-TCO/SF_{Tz}08* treatment produced crisp fluorescent mitochondrial images with an exceptional resolution (Figure 11b,e,j). Plot intensity values of pixels along a red line (Figure 11c,d) revealed a sharp contrast between the mitochondrion and other areas, which validated complete fluorescence quenching of SF_{Tz}s under the physiological culture-media condition (zero intensity was observed in the extracellular area). To confirm the selectivity of TPP-TCO/SF_{Tz}02* and TPP-TCO/SF_{Tz}08* for mitochondria, HeLa cells were cotreated with commercially available mitochondria staining dye MitoTracker Deep Red, and we observed excellent colocalization of the signal between MitoTracker Deep Red and SF_{Tz}02* or SF_{Tz}08*. Together, highly efficient and selective fluorescent staining of intracellular TOI protein and intracellular organelles was possible without multiple washing steps using SF_{Tz}s in live cell conditions.

CONCLUSION

In summary, the monochromophoric design strategy enables the development of fluorogenic probe SF_{Tz}s, having an extraordinary turn-on/off ratio covering the full visible color range, for the live cell imaging via rapid and catalyst-free bioorthogonal reaction. Strong electronic coupling between the SF core and Tz

DOI: 10.1021/jacs.7b10433
J. Am. Chem. Soc. 2018, 140, 974−983

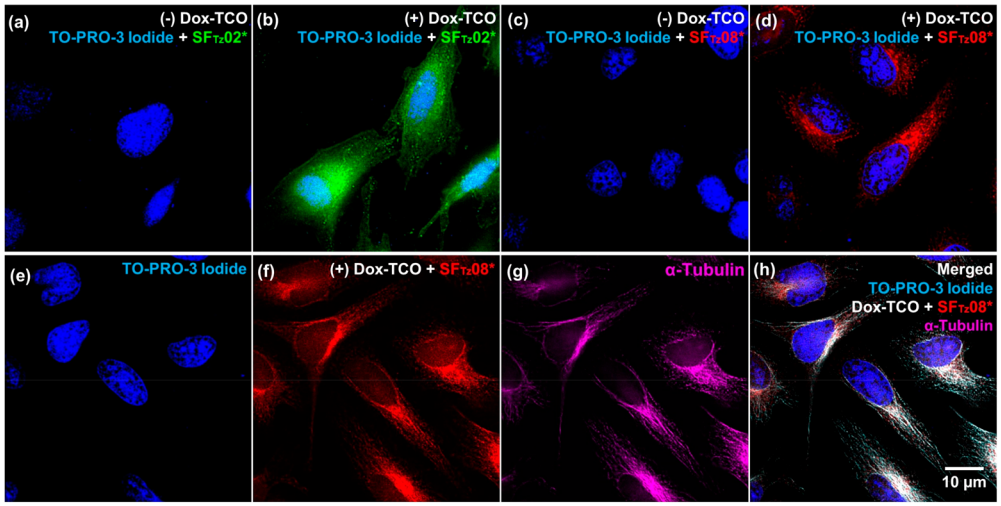

Figure 10. Fluorogenic bioorthogonal imaging of innate microtubules with SF_{Tz} in a fixed-cell condition. HeLa human cervical carcinoma cells were treated with DMSO (a, c) or Dox-TCO (b, d) for 1 h. TO-PRO-3 iodide (1 μM) was used for nucleus staining. After a brief washing with PBS, $SF_{Tz}02^*$ (a, b) or $SF_{Tz}08^*$ (c, d) was used to treat the cells (final concentration = 10 μM). Immediately after addition of the probes, the cell images were observed with a fluorescence microscope without washing. Selective microtubule staining was further confirmed with immunofluorescence using α-tubulin antibody (g–h). Scale bar, 10 μm.

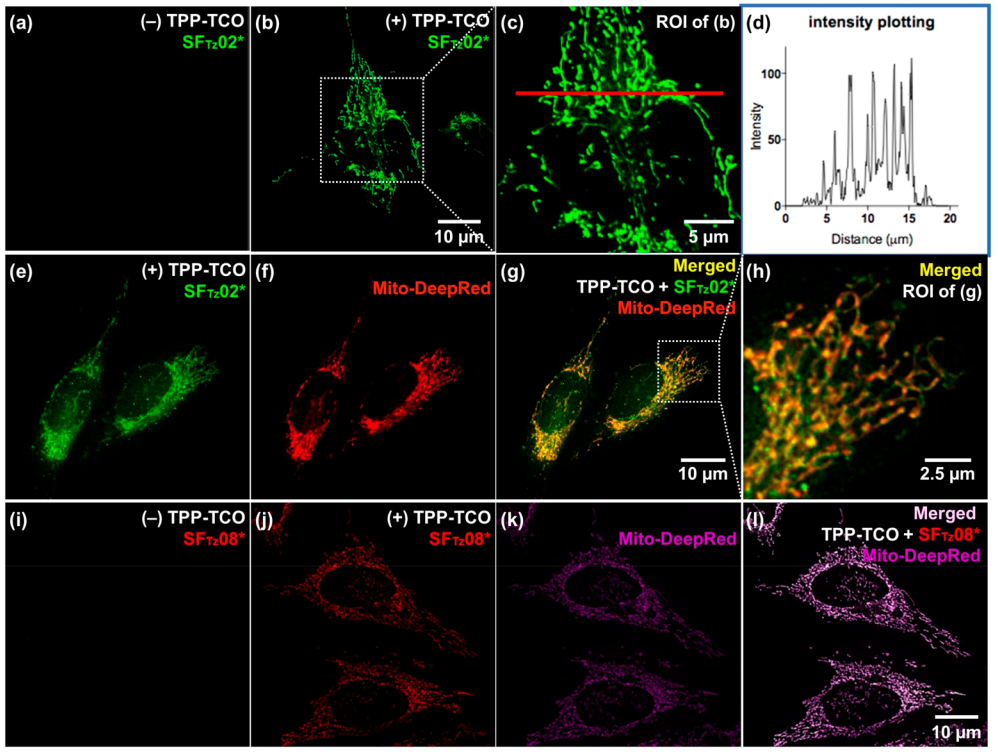

Figure 11. Fluorogenic bioorthogonal imaging of mitochondria with $SF_{Tz}02^*$ and $SF_{Tz}08^*$ in live cell conditions without washing steps. HeLa human cervical carcinoma cells were treated with DMSO (a, i) or triphenylphosphonium (TPP)–TCO (10 μM, b, c, e, g, h, j, l) with MitoTracker Deep Red (f–h, k, l) for 40 min. After brief washing with PBS, $SF_{Tz}02^*$ (a, b, c, e, g, h) or $SF_{Tz}08^*$ (i, j, l) were used to treat the cells (final concentration = 10 μM). Images were immediately observed with a fluorescence microscope without washing. (d) Plot intensity values of pixels along a red line in (c) were analyzed with the ImageJ program. ROI, region of interest.

chromophore causes dark-state quenching, which is completely different from the conventional FRET- or TBET-type energy transfer mechanism. Wavelength-independent dark-state quenching enables efficient widening of the emission color range of SF_{Tz}s, validating generality and robustness of this monochromophoric strategy. We successfully demonstrate an applicability of SF_{Tz}s for bioorthogonal fluorescent imaging of TOI proteins and subcellular organelles in live cell conditions without washing steps.

When applying this monochromophoric strategy, a dihydropyridazine moiety—product of TCO–Tz reaction—will directly affect the π-electronic system of the resulting fluorophores after the TCO–FL_{Tz} reaction. Considering photophysical properties of our monochromophoric probes, this group would act like

DOI: 10.1021/jacs.7b10433
J. Am. Chem. Soc. 2018, 140, 974–983

an electron withdrawing group (EWG). Therefore, our monochromophoric strategy will be suitable for fluorophores having specific positions, where an EWG is essential to exhibit fluorescent properties. In this regard, the EWG position of charge-transfer-type fluorophores, such as nitrobenzoxadiazole (NBD), acedan, or coumarin derivatives, might be a potential candidate for tetrazine incorporation. We believe the monochromophoric design strategy will be useful to provide a highly reliable and generally applicable method for the development of bioorthogonal fluorogenic probes with excellent turn-on/off ratio *in vitro* and *in vivo*.

■ ASSOCIATED CONTENT

Supporting Information

The Supporting Information is available free of charge on the ACS Publications website at DOI: 10.1021/jacs.7b10433.

General experimental information, supporting figures, experimental procedure for live cell fluorescence image, ^{1}H and ^{13}C spectra of new compounds, references (PDF)

■ AUTHOR INFORMATION

Corresponding Authors

*ehkim01@ajou.ac.kr
*sbpark@snu.ac.kr

ORCID

Wansang Cho: 0000-0002-5262-9543
Seung Bum Park: 0000-0003-1753-1433

Notes

The authors declare no competing financial interest.

■ ACKNOWLEDGMENTS

This work was supported by the Creative Research Initiative Grant (2014R1A3A2030423), Bio & Medical Technology Development Program (2012M3A9C4048780), and Basic Research Program (2009-0093826 and 2016R1C1B2014699) through the National Research Foundation of Korea (NRF) funded by the Korean Government (Ministry of Science & ICT). Y.L. is grateful for his predoctoral fellowship awarded by the BK21 Plus Program. W.C. is grateful for the NRF-2016-Fostering Core Leaders of the Future Basic Science Program/Global Ph.D. Fellowship Program (2016H1A2A1908141).

■ REFERENCES

(1) (a) Fernández-Suárez, M.; Ting, A. Y. *Nat. Rev. Mol. Cell Biol.* **2008**, *9*, 929−943. (b) Hell, S. W. *Nat. Methods* **2009**, *6*, 24−32.

(2) (a) Lavis, L. D.; Raines, R. T. *ACS Chem. Biol.* **2008**, *3*, 142−155. (b) Lavis, L. D.; Raines, R. T. *ACS Chem. Biol.* **2014**, *9*, 855−866. (c) Dean, K. M.; Palmer, A. E. *Nat. Chem. Biol.* **2014**, *10*, 512−523.

(3) (a) Weissleder, R. *Nat. Biotechnol.* **2001**, *19*, 316−317. (b) Ntziachristos, V.; Ripoll, J.; Wang, L. V.; Weissleder, R. *Nat. Biotechnol.* **2005**, *23*, 313−320.

(4) (a) Chudakov, D. M.; Matz, M. V.; Lukyanov, S.; Lukyanov, K. A. *Physiol. Rev.* **2010**, *90*, 1103−1163. (b) Odell, I. D.; Cook, D. *J. Invest. Dermatol.* **2013**, *133*, e4.

(5) (a) van Dam, G. M.; Themelis, G.; Crane, L. M. A.; Harlaar, N. J.; Pleijhuis, R. G.; Kelder, W.; Sarantopoulos, A.; de Jong, J. S.; Arts, H. J. G.; van der Zee, A. G. J.; Bart, J.; Low, P. S.; Ntziachristos, V. *Nat. Med.* **2011**, *17*, 1315−1319. (b) Choi, H. S.; Gibbs, S. L.; Lee, J. H.; Kim, S. H.; Ashitate, Y.; Liu, F.; Hyun, H.; Park, G.; Xie, Y.; Bae, S.; Henary, M.; Frangioni, J. V. *Nat. Biotechnol.* **2013**, *31*, 148−153. (c) Xue, L.; Karpenko, I. A.; Hiblot, J.; Johnsson, K. *Nat. Chem. Biol.* **2015**, *11*, 917−923. (d) Kim, E.; Yang, K. S.; Kohler, R. H.; Dubach, J. M.; Mikula, H.; Weissleder, R. *Bioconjugate Chem.* **2015**, *26*, 1513−1518. (e) Lee, M. M.; Gao, Z.; Peterson, B. R. *Angew. Chem., Int. Ed.* **2017**, *56*, 6927−6931.

(6) Kim, E.; Yang, K. S.; Giedt, R. J.; Weissleder, R. *Chem. Commun.* **2014**, *50*, 4504−4507.

(7) (a) Sletten, E. M.; Bertozzi, C. R. *Angew. Chem., Int. Ed.* **2009**, *48*, 6974−6998. (b) Patterson, D. M.; Nazarova, L. A.; Prescher, J. A. *ACS Chem. Biol.* **2014**, *9*, 592−605.

(8) (a) Reiner, T.; Earley, S.; Turetsky, A.; Weissleder, R. *ChemBioChem* **2010**, *11*, 2374−2377. (b) Cserép, G. B.; Herner, A.; Kele, P. *Methods Appl. Fluoresc.* **2015**, *3*, 042001.

(9) Oliveira, B. L.; Guo, Z.; Bernardes, G. J. L. *Chem. Soc. Rev.* **2017**, *46*, 4895−4950.

(10) (a) Blackman, M. L.; Royzen, M.; Fox, J. M. *J. Am. Chem. Soc.* **2008**, *130*, 13518−13519. (b) Devaraj, N. K.; Weissleder, R.; Hilderbrand, S. A. *Bioconjugate Chem.* **2008**, *19*, 2297−2299. (c) Taylor, M. T.; Blackman, M. L.; Dmitrenko, O.; Fox, J. M. *J. Am. Chem. Soc.* **2011**, *133*, 9646−9649. (d) Knall, A.-C.; Slugovc, C. *Chem. Soc. Rev.* **2013**, *42*, 5131−5142. (e) Selvaraj, R.; Fox, J. M. *Curr. Opin. Chem. Biol.* **2013**, *17*, 753−760. (f) Mayer, S.; Lang, K. *Synthesis* **2017**, *49*, 830−848.

(11) (a) Devaraj, N. K.; Hilderbrand, S.; Upadhyay, R.; Mazitschek, R.; Weissleder, R. *Angew. Chem., Int. Ed.* **2010**, *49*, 2869−2872. (b) Carlson, J. C. T.; Meimetis, L. G.; Hilderbrand, S. A.; Weissleder, R. *Angew. Chem., Int. Ed.* **2013**, *52*, 6917−6920. (c) Wu, H.; Yang, J.; Šečkutė, J.; Devaraj, N. K. *Angew. Chem., Int. Ed.* **2014**, *53*, 5805−5809. (d) Meimetis, L. G.; Carlson, J. C. T.; Giedt, R. J.; Kohler, R. H.; Weissleder, R. *Angew. Chem., Int. Ed.* **2014**, *53*, 7531−7534. (e) Knorr, G.; Kozma, E.; Herner, A.; Lemke, E. A.; Kele, P. *Chem. - Eur. J.* **2016**, *22*, 8972−8979. (f) Wieczorek, A.; Werther, P.; Euchner, J.; Wombacher, R. *Chem. Sci.* **2017**, *8*, 1506−1510. (g) Kozma, E.; Estrada Girona, G.; Paci, G.; Lemke, E. A.; Kele, P. *Chem. Commun.* **2017**, *53*, 6696−6699.

(12) (a) Budin, G.; Yang, K. S.; Reiner, T.; Weissleder, R. *Angew. Chem., Int. Ed.* **2011**, *50*, 9378−9381. (b) Yang, K. S.; Budin, G.; Reiner, T.; Vinegoni, C.; Weissleder, R. *Angew. Chem., Int. Ed.* **2012**, *51*, 6598−6603.

(13) (a) Förster, T. *Ann. Phys.* **1948**, *2*, 55−75. (b) Förster, T. *Discuss. Faraday Soc.* **1959**, *27*, 7−17.

(14) Jiao, G.-S.; Thoresen, L. H.; Burgess, K. *J. Am. Chem. Soc.* **2003**, *125*, 14668−14669. (b) Bandichhor, R.; Petrescu, A. D.; Vespa, A.; Kier, A. B.; Schroeder, F.; Burgess, K. *J. Am. Chem. Soc.* **2006**, *128*, 10688−10689.

(15) (a) Dexter, D. L. *J. Chem. Phys.* **1953**, *21*, 836−850. (b) Otsuki, J.; Kanazawa, Y.; Kaito, A.; Islam, D.-M. S.; Araki, Y.; Ito, O. *Chem. - Eur. J.* **2008**, *14*, 3776−3784. (c) Hurenkamp, J. H. Tuning Energy Transfer between Chromophores Switchable Molecular Photonic Systems. Ph.D. Thesis, University of Groningen, 2008.

(16) (a) Kim, E.; Koh, M.; Ryu, J.; Park, S. B. *J. Am. Chem. Soc.* **2008**, *130*, 12206−12207. (b) Kim, E.; Koh, M.; Lim, B. J.; Park, S. B. *J. Am. Chem. Soc.* **2011**, *133*, 6642−6649. (c) Lee, Y.; Na, S.; Lee, S.; Jeon, N. L.; Park, S. B. *Mol. BioSyst.* **2013**, *9*, 952−956. (d) Choi, E. J.; Kim, E.; Lee, Y.; Jo, A.; Park, S. B. *Angew. Chem., Int. Ed.* **2014**, *53*, 1346−1350. (e) Kim, E.; Lee, Y.; Lee, S.; Park, S. B. *Acc. Chem. Res.* **2015**, *48*, 538−547.

(17) (a) Anslyn, E. V.; Dougherty, D. A. *Modern Physical Organic Chemistry*; University Science Books: Sausalito, CA. 2005. (b) Turro, N. J.; Ramamurthy, V.; Scaiano, J. C. *Principles of Molecular Photochemistry: An Introduction*, 1st ed.; University Science Books: Sausalito, CA, 2008.

(18) (a) Gong, Y.-H.; Miomandre, F.; Méallet-Renault, R.; Badré, S.; Galmiche, L.; Tang, J.; Audebert, P.; Clavier, G. *Eur. J. Org. Chem.* **2009**, *2009*, 6121−6128. (b) Clavier, G.; Audebert, P. *Chem. Rev.* **2010**, *110*, 3299−3314.

(19) Escudero, D. *Acc. Chem. Res.* **2016**, *49*, 1816−1824.

(20) Plugge, M.; Alain-Rizzo, V.; Audebert, P.; Brouwer, A. M. *J. Photochem. Photobiol., A* **2012**, *234*, 12−20.

(21) Yang, J.; Karver, M. R.; Li, W.; Sahu, S.; Devaraj, N. K. *Angew. Chem., Int. Ed.* **2012**, *51*, 5222−5225.

(22) (a) Presolski, S. I.; Hong, V.; Cho, S.-H.; Finn, M. G. *J. Am. Chem. Soc.* **2010**, *132*, 14570−14576. (b) Lang, K.; Chin, J. W. *ACS Chem. Biol.* **2014**, *9*, 16−20.

DOI: 10.1021/jacs.7b10433
J. Am. Chem. Soc. 2018, 140, 974−983

(23) (a) Song, W.; Wang, Y.; Qu, J.; Lin, Q. *J. Am. Chem. Soc.* **2008**, *130*, 9654−9655. (b) Song, W.; Wang, Y.; Qu, J.; Madden, M. M.; Lin, Q. *Angew. Chem., Int. Ed.* **2008**, *47*, 2832−2835. (c) Yu, Z.; Pan, Y.; Wang, Z.; Wang, J.; Lin, Q. *Angew. Chem., Int. Ed.* **2012**, *51*, 10600−10604.
(24) Hansch, C.; Leo, A.; Taft, R. W. *Chem. Rev.* **1991**, *91*, 165−195.
(25) (a) Adamo, C.; Jacquemin, D. *Chem. Soc. Rev.* **2013**, *42*, 845−856. (b) Liu, X.; Qiao, Q.; Tian, W.; Liu, W.; Chen, J.; Lang, M. J.; Xu, Z. *J. Am. Chem. Soc.* **2016**, *138*, 6960−6963.
(26) (a) Kasha, M. *Discuss. Faraday Soc.* **1950**, *9*, 14−19. (b) Klán, P.; Wirz, J. *Photochemistry of Organic Compounds: From Concepts to Practice*; Wiley-Blackwell, 2009.
(27) (a) Hilborn, R. C. *Am. J. Phys.* **1982**, *50*, 982−986. (b) Lee, Y.; Jo, A.; Park, S. B. *Angew. Chem., Int. Ed.* **2015**, *54*, 15689−15693. (c) Valeur, B.; Berberan-Santos, M. N. *Molecular Fluorescence: Principles and Applications*, 2nd ed.; Wiley-VCH: Weinheim, 2012.
(28) Alirol, E.; Martinou, J. C. *Oncogene* **2006**, *25*, 4706−4716.

DOI: 10.1021/jacs.7b10433
J. Am. Chem. Soc. 2018, 140, 974−983